

# Hall drift of fractional Chern insulators in few-boson systems

C. Repellin,<sup>1,\*</sup> J. Léonard,<sup>2</sup> and N. Goldman<sup>3,†</sup>

<sup>1</sup>Univ. Grenoble-Alpes, CNRS, LPMCM, 38000 Grenoble, France

<sup>2</sup>Department of Physics, Harvard University, Cambridge, Massachusetts 02138, USA

<sup>3</sup>CENOLI, Université Libre de Bruxelles, CP 231, Campus Plaine, B-1050 Brussels, Belgium

(Dated: June 3, 2022)

Detecting signatures of fractional quantum Hall states in few-particle systems remains an outstanding challenge. In this work, we numerically analyze the center-of-mass Hall drift of a small ensemble of hardcore bosons, initially prepared in the ground state of the Harper-Hofstadter-Hubbard model. By extracting the Hall conductivity in a wide range of the magnetic flux, we identify an emergent “Hall plateau” compatible with a fractional Chern insulator state, whose width agrees with the spectral and topological properties of the prepared ground state. Our calculations suggest that fractional Chern insulators can be detected in cold-atom experiments, using available detection methods.

**Introduction.** Important progress is being made in view of realizing and detecting strongly-correlated topological phases of ultracold atoms in optical lattices [1, 2]. On the one hand, experimental efforts have been dedicated to the creation of artificial gauge fields [3, 4] and topological Bloch bands [2] for neutral atomic gases, leading to concrete measurements of topological properties [5–21]. On the other hand, theoretical studies have identified realistic schemes for preparing and stabilizing small atomic ensembles in fractional Chern insulators (FCI) [22–29], which are lattice analogues of fractional quantum Hall (FQH) liquids [30, 31]; they also proposed methods to probe their main characteristic features [32–40]. This progress should soon lead to the realization of FCIs in small atomic ensembles, and to the possibility of observing their properties. However, identifying clear and accessible topological signatures of FCIs in small interacting atomic systems still constitutes a central challenge. In fact, this question concerns a wide range of quantum-engineered platforms, including strongly-interacting photonic systems [41–43].

The canonical signature of FQH states is provided by the Hall conductivity, i.e. the linear-response coefficient relating an induced transverse current to the applied force. In the FQH effect, the Hall conductivity is quantized to a value  $\sigma_H/\sigma_0 \in \mathbb{Q}$  in the thermodynamic limit [44];  $\sigma_0^{-1} = R_K$  is von Klitzing’s constant. The Hall response is also accessible in ultracold atoms; it has been measured in weakly-interacting gases through various schemes, including center-of-mass drifts [6, 17, 21, 45–47] and local currents [20, 48], and more indirectly, through collective-mode excitations [49] and circular dichroism [18]. Whether the Hall response could be used to detect FCIs in few-body systems remains an important question to be addressed.

In this Letter, we numerically analyze the Hall drift of a small ensemble of strongly-interacting (hardcore) bosons, initially prepared in the ground state of the Harper-Hofstadter-Hubbard model [50, 51]. Building on Refs. [6, 52], we monitor the center-of-mass of the prepared state upon releasing it into a larger lattice while applying a weak static force. This Hall drift measurement, which provides an estimation of the Hall conductivity in the prepared state, is performed in a wide range of magnetic flux values [Fig. 1]. We identify a win-

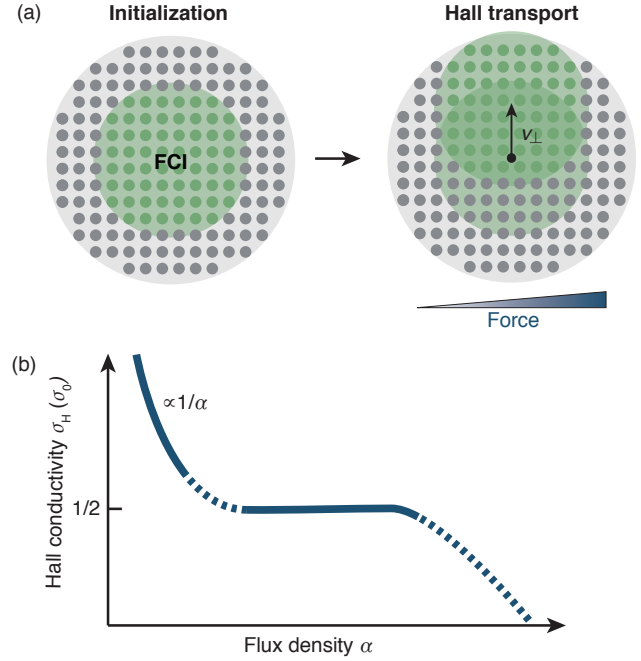


Figure 1. (a) The Hall drift protocol: The prepared FCI state is released into a larger lattice and a uniform force is applied. The Hall conductivity is extracted from the center-of-mass drift transverse to the force. (b) Sketch of the Hall conductivity  $\sigma_H(\alpha)$  as a function of the flux density in the Harper-Hofstadter-Hubbard (HHH) model. In the continuum limit  $\alpha \ll 1$ , the system follows the classical prediction  $\sigma_H = \rho/\alpha$ , where  $\rho$  is the particle density. In the vicinity of the filling factor  $\nu = \rho/\alpha = 1/2$ , a fractional Chern insulator (FCI) is formed and  $\sigma_H(\alpha)$  depicts a plateau in the thermodynamic limit.

dow of decreased sensitivity to the magnetic flux, reminiscent of the Hall plateaus that are expected in the thermodynamic limit, where the extracted Hall conductivity is compatible with finite-size estimations of the many-body Chern number [40]. This window coincides with the region where we identify an FCI ground state through entanglement spectroscopy. Our results indicate that FCI states composed of few bosons ( $N \geq 3$ ) can be identified through Hall drifts under realistic experimental conditions.

*The Hall drift protocol.* In this work, we numerically extract the Hall conductivity  $\sigma_H$  from the center-of-mass drift of an initially prepared state upon applying a weak external force. This center-of-mass probe [6, 52, 53] is particularly suitable when considering a very small ensemble of particles, for which local currents substantially fluctuate. Besides, in order to limit boundary effects, we release the initially prepared state into a larger lattice [52, 54] before monitoring the center-of-mass drift. This protocol is implementable in cold-atom experiments, where tunneling can be dynamically tuned and center-of-mass motion measured [6, 17, 21, 45–47]. In our simulations, the time scales associated with the progressive release of the inner system, as well as the duration of the Hall-drift measurement, are adjusted to avoid boundary effects due to the outer edge (i.e. the finite simulation box).

The center-of-mass drift transverse to the applied force  $F$ , i.e. the Hall drift  $x_\perp(t)$ , allows one to extract the Hall velocity  $v_\perp = x_\perp(t)/t$ , upon reaching a stationary regime within linear response. This center-of-mass Hall velocity is related to the transverse current density through the relation  $v_\perp = j_\perp/\rho$ , where  $\rho$  denotes the particle density. From the transport equation,  $j_\perp = \sigma_H F$ , one extracts the Hall conductivity through the relation  $\sigma_H = (\rho/F)v_\perp$ . Setting  $\hbar = 1$ , the conductivity quantum reads  $\sigma_0 = (1/2\pi)$ , so that  $\sigma_H/\sigma_0 = (2\pi\rho/F)v_\perp$ .

For a translationally-invariant quantum system consisting of  $N$  interacting particles moving in a uniform magnetic field, the center-of-mass dynamics are independent of the interaction strength [55–57] and the Hall conductivity follows the classical (Drude) prediction,  $\sigma_H/\sigma_0 = \rho/\alpha$ , where  $\alpha$  denotes the number of flux quanta ( $\Phi_0 = 2\pi$ ) per unit area. In this setting, the Hall velocity reads  $v_\perp = F/2\pi\alpha$ , and thus, it does not depend on the particle number  $N$ . This classical behavior breaks down upon breaking translational symmetry (e.g. by adding a lattice, disorder or an edge [58]), hence opening the possibility for quantized Hall plateaus  $\sigma_H/\sigma_0 = \nu_{\text{Ch}}^{\text{MB}} \in \mathbb{Q}$  around filling factors that correspond to incompressible states [44, 57]; here the quantity  $\nu_{\text{Ch}}^{\text{MB}}$  denotes the many-body Chern number, a topological invariant associated with the ground-state of the many-body system [59, 60].

*Microscopic model and ground-state properties.* In this work, we study the emergence of quantized Hall plateaus in the center-of-mass dynamics of strongly-interacting bosons moving on a 2D square lattice in the presence of a uniform flux per plaquette. The corresponding Harper-Hofstadter-Hubbard (HHH) Hamiltonian reads [50, 51]

$$\hat{H}_0 = -J \left( \sum_{m,n} \hat{a}_{m,n+1}^\dagger \hat{a}_{m,n} + e^{i2\pi\alpha n} \hat{a}_{m+1,n}^\dagger \hat{a}_{m,n} + \text{h.c.} \right) + (U/2) \sum_m \hat{a}_{m,n}^\dagger \hat{a}_{m,n} (\hat{a}_{m,n}^\dagger \hat{a}_{m,n} - 1), \quad (1)$$

where  $\hat{a}_{m,n}^\dagger$  creates a boson at lattice site  $(m, n)$ ,  $J$  denotes the tunneling amplitude,  $U$  is the on-site (Hubbard) interaction strength [61], and where the Peierls phase factors [50] account for the presence of a flux  $\Phi = 2\pi\alpha$  per plaquette.

This model has been implemented in ultracold-atom experiments [62] using Floquet engineering [1, 2].

Numerical simulations using periodic boundary conditions have established that the HHH model hosts a bosonic FCI akin to the Laughlin state [44], for strongly repulsive interactions and filling factor  $\nu = \rho/\alpha = 1/2$ ; see Refs. [26–28, 32, 51, 63]. For hardcore bosons, these calculations reveal a stable FCI ground state for  $\alpha \leq 0.3$ ; the bulk gap is maximal around  $\alpha \approx 0.2 - 0.25$  [28, 51, 63], and vanishes in the limit  $\alpha \ll 1$ . This FCI is characterized by a fractional many-body Chern number,  $\nu_{\text{Ch}}^{\text{MB}} = 1/2$ , which the Hall conductivity approaches in the thermodynamic limit [40]. For large enough systems, these results are expected to be independent of geometry and boundary conditions. In few-body systems, however, where boundary effects are important, the FCI phase may exist in a different range of  $\rho$  and  $\alpha$ , or may even not be stable.

In our Hall-drift calculations, we consider  $N$  hardcore bosons initially confined in a circular box containing  $N_s$  lattice sites [Fig. 1(a)]. As a first step, we analyze the ground-state properties of this few-body system in view of determining the values of  $\rho$  and  $\alpha$  that realize a  $\nu = 1/2$  FCI state; we will see that this parameter regime is far from the thermodynamic-limit expectation ( $\rho/\alpha = 1/2$ ). We can first gain some intuition from the physics of the FQH effect in the (continuum) disk geometry. For a flux density  $\alpha \leq 0.3$ , the lowest Bloch band of the single-particle Hofstadter spectrum contains a set of roughly  $N_0(\alpha)$  nearly degenerate states, which are connected to the next band by dispersive edge states [64]. These  $N_0(\alpha)$  states are analogous [33, 34] to the orbitals of the lowest Landau level (LLL) in the disk geometry; there, the  $\nu = 1/2$  Laughlin state with  $N$  bosons occupies  $2N - 1$  LLL orbitals [65]. Likewise, we may expect a  $\nu = 1/2$  FCI state when  $N_0(\alpha) \simeq 2N - 1$ .

We use exact diagonalization to verify the existence of the FCI ground state in our model, and specify its phase boundaries based on (i) the low-energy spectrum; (ii) entanglement spectroscopy; (iii) the occupation of single-particle orbitals. For concreteness, we analyse  $N = 4$  bosons in  $N_s = 60$  sites:

(i) Figure 2(a) shows the low-energy spectrum of this few-body system; there are three avoided crossings between the ground state and the first excited state within the range  $0 \leq \alpha \leq 0.3$ , which we interpret as the finite-size signatures of three phase transitions. We focus on the regime  $0.15 < \alpha < 0.25$ , where the expected FCI bulk gap is the largest [28, 51], and no phase transition is observed. In this regime, the approximate degeneracy of the lowest band,  $N_0(\alpha) \simeq 7$  [66], is compatible with an FCI ground state candidate for  $N = 4$ . We note that the nature of the phases at  $\alpha < 0.15$  is likely to be non-universal due to finite-size effects [67].

(ii) In finite geometries with edges, the topological nature of FCIs can be revealed through the degeneracies of their edge spectrum [33, 34]; however, this spectral signature requires a larger number of sites and a smooth confining potential [68]. Instead, we probe the bulk quasihole excitations of the ground state; their degeneracy is a topological fingerprint of the FCI phase, and it can be extracted from the ground state  $|\Psi_{\text{GS}}\rangle$  us-

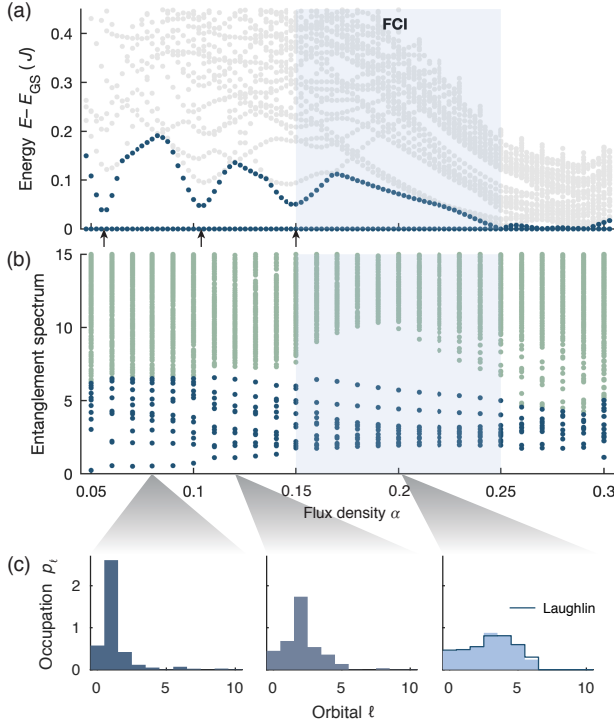


Figure 2. Static signatures of the strongly-correlated ground state, for  $N = 4$  hardcore bosons in the HHH model, in a circular box of  $N_s = 60$  sites. The FCI stability region (shaded) is indicated according to three markers: (a) Low-energy many-body spectrum (lowest 10 energies per discrete rotation-symmetry sector) relative to the ground-state energy  $E_{GS}$ . Analyzing absolute energies (not shown) reveals that the three local minima of the gap correspond to level crossings, which are avoided due to finite-size effects (arrows). (b) Particle entanglement spectrum (PES) for a bipartition with 2 particles in each subsystem. In the shaded region, the first 15 levels (blue) are well separated from the other levels, revealing that the ground state is topologically equivalent to the Laughlin state. (c) Occupation of the single-particle orbitals in the ground state (histograms) and in the exact Laughlin state on the disk (line). The orbitals are sorted in increasing energy and angular momentum, respectively.

ing the particle entanglement spectrum [69] (PES). The PES is the spectrum of the reduced density matrix obtained by tracing  $|\Psi_{GS}\rangle \langle \Psi_{GS}|$  over a bipartition containing  $N_A$  particles, while keeping the geometry of the system intact. The degeneracy of Laughlin quasiholes is determined through a generalized exclusion principle [70]; for 2 bosons in 7 orbitals, it is 15-fold. And indeed, for  $0.15 < \alpha < 0.25$  and  $N_A = 2$ , the PES in Fig. 2(b) reveals a clear gap above the 15th state, which confirms the FCI nature of  $|\Psi_{GS}\rangle$  in this parameter range.

(iii) To further characterize the ground state, we calculated the occupation of each single-particle orbital. For the Laughlin state on the disk, there is a uniform occupation of all  $2N - 1$  orbitals in the thermodynamic limit, with moderate deviations from this distribution for small systems. We find a similar distribution in the regime  $0.15 \lesssim \alpha \lesssim 0.25$  for the same number of particles [Fig. 2(c)].

Overall, the two probes offered by entanglement and

occupation-number properties consistently reveal that the ground state is in the  $\nu = 1/2$  FCI phase within the range  $0.15 \lesssim \alpha \lesssim 0.25$ . We have verified that these results are robust with respect to changes in the particle number ( $N = 3, 4$ ) and number of sites  $N_s$ ; see [66]. For fixed  $N$ , a moderate increase of  $N_s$  moves the position of each phase transition to smaller values of  $\alpha$ ; indeed, keeping  $N_0(\alpha)$  constant and equal to  $2N - 1$  while increasing  $N_s$  requires decreasing  $\alpha$ . This behavior suggests the existence of an optimal value for the particle density  $\rho$  such that the flux density of optimal bulk gap (for constant  $\nu = 1/2$ ) falls in the middle of the FCI stability region (as evaluated for constant  $\rho$ ).

*Benchmark using non-interacting fermions.* We first benchmark the Hall-drift measurement by considering non-interacting fermions in the Harper-Hofstadter model, at quarter filling  $\rho = 1/4$ . In this setting, (integer) Chern insulators are expected at flux densities  $\alpha = 1/(4n)$ , with  $n \in \mathbb{Z}$ , where they exhibit quantized Hall plateaus  $\sigma_H/\sigma_0 = n$  in the thermodynamic limit, upon small variations of the flux  $\alpha$ . While this result can be directly deduced from a Diophantine equation [71, 72], the actual size of these plateaus follows a rather complicated law established by the underlying single-particle (Hofstadter-butterfly) spectrum [50]. Furthermore, such Hall plateaus can be altered by finite-size effects. This first numerical study aims to shed some light on these properties.

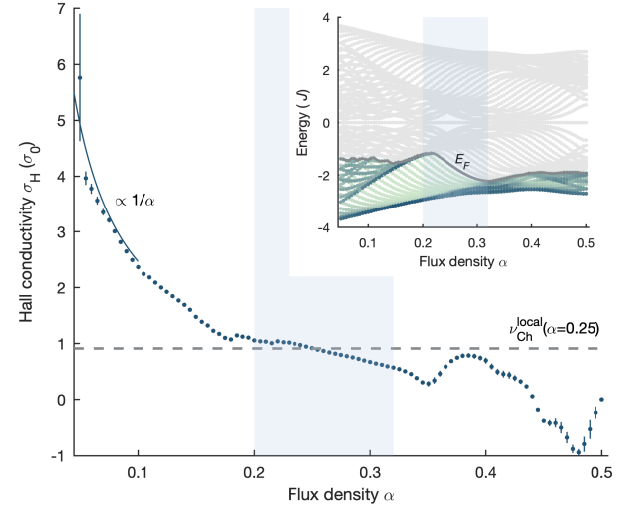


Figure 3. Benchmark using non-interacting fermions: Hall conductivity extracted from the Hall drift of  $N = 20$  fermions, initially prepared in a small circular box of  $N_s = 81$  sites (i.e. quarter filling); the release into the larger system (1005 sites) and the ramping up of the force ( $F = 0.2J/d$ ) are performed over a duration  $\tau_{ramp} = 15J^{-1}$ , and the Hall drift measurement over  $\tau_{hold} = 13J^{-1}$ ;  $\nu_{Ch}^{local}$  denotes the local real-space Chern number; fit error bars reflect the 95% confidence interval. (Inset) Single-particle spectrum  $E(\alpha)$ , for the same box (81 sites); the Fermi level ( $E_F$ ; grey curve) corresponds to the same  $N = 20$ ; filled states are colored in green (bulk states are dark and edge states are light), while empty states are grey;  $E_F$  is located in the main bulk gap (Chern insulator) within the shaded region.

We determine the Hall drift by calculating the time-evolution of  $N = 20$  non-interacting fermions, initially pre-

pared in the ground-state of the Harper-Hofstadter model within a circular box of  $N_s = 81$  sites ( $\rho \approx 1/4$ ), which are then released into a larger lattice (1005 sites) and subjected to a weak force  $F = 0.2J/d$ , where  $d$  is the lattice spacing [66]. The Hall conductivity extracted from the stationary (linear-response) Hall drift is depicted as a function of the flux density in Fig. 3. In the low-flux regime ( $\alpha \lesssim 0.1$ ), lattice effects are negligible and the Hall drift follows the classical prediction  $\sigma_H/\sigma_0 = \rho/\alpha$ . At  $\alpha = 0.25$ , the Fermi energy lies within the first bulk gap of the spectrum, which yields an approximately quantized value  $\sigma_H/\sigma_0 \approx 0.91$ , dictated by the Chern number  $\nu_{\text{Ch}} = 1$  of the fully occupied Bloch band [71]; we have verified that this measured  $\sigma_H$  matches the average value of the local real-space Chern number [73, 74], as evaluated over 29 sites in the prepared ground state. The Hall response remains approximately constant for a wide range of flux,  $\alpha \in [0.2, 0.32]$ , in agreement with the Fermi level's location within the main bulk gap of the underlying spectrum [Fig. 3]; we verified that the flatness of this emergent Hall plateau, as well as the approached quantized value, improve as the system size  $N_s$  increases. These results illustrate how the Hofstadter-butterfly spectrum dictates the size of emergent Hall plateaus in realistic finite-size (non-interacting) settings.

*Hall drift analysis for interacting bosons.* We now turn to the Hall drift of hardcore bosons. A system of  $N = 4$  bosons is initially prepared in the ground state of the HHH model, using a circular box of  $N_s = 60$  sites. At  $t = 0$ , this bosonic cloud is then slowly released into a larger circle (124 sites), while the force is ramped up to the value  $F = 0.01J/d$ ; see [66] for details on the ramps used in view of reaching a stationary regime. Our numerics show that a stationary center-of-mass motion takes place after the ramp, during a time window of a few tunneling times [Fig. 4(b)], from which we extract the (constant) Hall velocity  $v_\perp$ . For longer times, the center-of-mass motion is affected by the edge of the large circle (i.e. the finite simulation box), which sets the end of the stationary regime; we point out that this numerical constraint is not an experimental one, since the prepared state can be released into a much larger lattice in realistic setups to prolong the stationary regime.

We extract the Hall conductivity from the stationary Hall velocity for a large range of flux values  $\alpha$ ; see Fig. 4. First, we find that the classical behavior  $\sigma_H/\sigma_0 = \rho/\alpha$  is recovered [75] in the low-flux (continuum) limit [Fig. 4(c)]. The correlated behavior of our interacting system then appears for  $\alpha \geq 0.1$  [Fig. 4(a)]. Most strikingly,  $\sigma_H(\alpha)$  shows clear inflections at the two values of  $\alpha$  that determine the boundaries of the  $\nu = 1/2$  FCI phase [Fig. 2]. Within this flux window,  $\sigma_H$  exhibits a reduced sensitivity, suggesting an emergent plateau related to the FCI state. In this regime, the value of  $\sigma_H$  is compatible with the finite-size many-body Chern number (0.294 for 4 bosons at  $\alpha = 0.25$ ), which was calculated in the torus geometry [40]. This emergent plateau is expected to be further accentuated in the thermodynamic limit, in view of forming a quantized plateau at the value  $\sigma_H/\sigma_0 = 0.5$ .

We have simulated our Hall drift protocol for various sys-

tem sizes  $N_s$ , considering  $N = 3, 4$  bosons [66]. Our results show that the  $\nu = 1/2$  FCI state can be detected by measuring the center-of-mass Hall drift of systems as small as 3 bosons in  $N_s = 40$  sites and 4 bosons in  $N_s = 49$  sites.

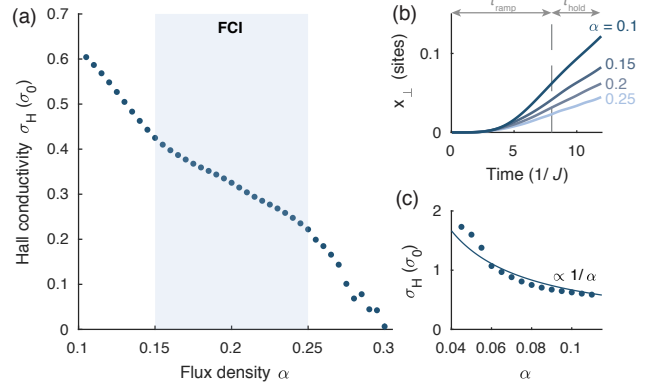


Figure 4. Hall drift of hardcore bosons in the HHH model [Eq. (1)]. After preparation in the ground state, 4 bosons confined in a circular box ( $N_s = 60$ ) are progressively released into a larger circle containing 124 sites and subjected to a uniform force  $F = 0.01J/d$ . At the end of this ramp, the center-of-mass motion is stationary for a few tunneling times [panel (b)], permitting the extraction of the Hall conductivity [panel (a)]; fit error bars (95% confidence) are smaller than the dots. The boundaries of the FCI phase (shaded region from Fig. 2) coincide with the inflection points delimiting the region of decreased sensitivity of  $\sigma_H(\alpha)$ . (c) Classical regime at low flux  $\alpha \ll 1$ .

*Concluding experimental considerations.* For a possible implementation of the proposed protocol, we consider the following experimental scheme. First, the FCI is prepared through adiabatic quantum state engineering, starting from a topologically trivial state that undergoes a topological phase transition to an FCI by slowly tuning the Hamiltonian parameters [24–29]. The adiabaticity of this preparation relies on the finite extent of the system, which prevents the many-body gap from vanishing at the transition point. In our scheme, the FCI would be embedded in a lattice with more sites, which are initially uncoupled either by switching off the tunneling to those sites (as assumed in our numerical calculations), or by increasing their energy with a repulsive potential. The drift protocol is initiated by restoring the coupling to outer sites and simultaneously ramping up a force induced by, for instance, an optical or magnetic potential gradient [6, 46]. Finally, the Hall drift is detected by measuring the center-of-mass position after variable drift times. Detecting center-of-mass displacements smaller than one lattice site, as depicted in Fig. 4, is within the current capabilities of cold-atom experiments [62]. Yet, we expect that even stronger signatures are possible because experiments allow access to total system sizes and drift times beyond the reach of exact numerics. In addition, the ability to choose finite interactions and to tune them dynamically opens up the possibility for advanced transport studies. The simplicity of this realistic experimental scheme paves the way to the exploration of quantum transport in strongly-correlated ultracold topological matter.

During completion of our manuscript, we became aware of a recent work [76], which also analyses the Hall response of an FCI in the HHH model.

**Acknowledgments** We thank M. Greiner for insightful discussions. We acknowledge J. Motruk and I. Na for sharing their manuscript [76] before submission, and for their comments on our work. C.R. is supported by the Marie Skłodowska-Curie program under EC Grant agreement 751859. J. L. acknowledges support from the Swiss National Science Foundation. N.G. is supported by the FRS-FNRS (Belgium) and the ERC Starting Grant TopoCold.

---

\* cecile.repellin@lpmmc.cnrs.fr

† ngoldman@ulb.ac.be

- [1] N. Goldman, J. C. Budich, and P. Zoller, “Topological quantum matter with ultracold gases in optical lattices,” *Nature Physics*, vol. 12, pp. 639–645, July 2016.
- [2] N. Cooper, J. Dalibard, and I. Spielman, “Topological bands for ultracold atoms,” *Reviews of Modern Physics*, vol. 91, no. 1, p. 015005, 2019.
- [3] J. Dalibard, F. Gerbier, G. Juzeliūnas, and P. Öhberg, “Colloquium: Artificial gauge potentials for neutral atoms,” *Reviews of Modern Physics*, vol. 83, pp. 1523–1543, Nov 2011.
- [4] N. Goldman, G. Juzeliūnas, P. Öhberg, and I. B. Spielman, “Light-induced gauge fields for ultracold atoms,” *Reports on Progress in Physics*, vol. 77, p. 126401, Dec. 2014.
- [5] M. Atala, M. Aidelsburger, J. T. Barreiro, D. Abanin, T. Kitagawa, E. Demler, and I. Bloch, “Direct measurement of the Zak phase in topological Bloch bands,” *Nature Physics*, vol. 9, no. 12, pp. 795–800, 2013.
- [6] M. Aidelsburger, M. Lohse, C. Schweizer, M. Atala, J. T. Barreiro, S. Nascimbène, N. R. Cooper, I. Bloch, and N. Goldman, “Measuring the Chern number of Hofstadter bands with ultracold bosonic atoms,” *Nature Physics*, vol. 11, pp. 162–166, Feb. 2015.
- [7] S. Nakajima, T. Tomita, S. Taie, T. Ichinose, H. Ozawa, L. Wang, M. Troyer, and Y. Takahashi, “Topological Thouless pumping of ultracold fermions,” *Nature Physics*, vol. 12, no. 4, pp. 296–300, 2016.
- [8] M. Lohse, C. Schweizer, O. Zilberberg, M. Aidelsburger, and I. Bloch, “A Thouless quantum pump with ultracold bosonic atoms in an optical superlattice,” *Nature Physics*, vol. 12, no. 4, pp. 350–354, 2016.
- [9] Z. Wu, L. Zhang, W. Sun, X.-T. Xu, B.-Z. Wang, S.-C. Ji, Y. Deng, S. Chen, X.-J. Liu, and J.-W. Pan, “Realization of two-dimensional spin-orbit coupling for Bose-Einstein condensates,” *Science*, vol. 354, no. 6308, pp. 83–88, 2016.
- [10] W. Sun, C.-R. Yi, B.-Z. Wang, W.-W. Zhang, B. C. Sanders, X.-T. Xu, Z.-Y. Wang, J. Schmiedmayer, Y. Deng, X.-J. Liu, *et al.*, “Uncover topology by quantum quench dynamics,” *Physical Review Letters*, vol. 121, no. 25, p. 250403, 2018.
- [11] N. Fläschner, D. Vogel, M. Tarnowski, B. S. Rem, D.-S. Lühmann, M. Heyl, J. C. Budich, L. Mathey, K. Sengstock, and C. Weitenberg, “Observation of a dynamical topological phase transition,” *Nature Physics*, vol. 14, pp. 265–268, 2018.
- [12] M. Tarnowski, F. N. Ünal, N. Fläschner, B. S. Rem, A. Eckardt, K. Sengstock, and C. Weitenberg, “Measuring topology from dynamics by obtaining the Chern number from a linking number,” *Nature Communications*, vol. 10, no. 1, pp. 1–13, 2019.
- [13] S. Sugawa, F. Salces-Carcoba, A. R. Perry, Y. Yue, and I. Spielman, “Second Chern number of a quantum-simulated non-Abelian Yang monopole,” *Science*, vol. 360, no. 6396, pp. 1429–1434, 2018.
- [14] M. Lohse, C. Schweizer, H. M. Price, O. Zilberberg, and I. Bloch, “Exploring 4D quantum Hall physics with a 2D topological charge pump,” *Nature*, vol. 553, no. 7686, pp. 55–58, 2018.
- [15] E. J. Meier, F. A. An, A. Dauphin, M. Maffei, P. Massignan, T. L. Hughes, and B. Gadway, “Observation of the topological Anderson insulator in disordered atomic wires,” *Science*, vol. 362, no. 6417, pp. 929–933, 2018.
- [16] S. de Léséleuc, V. Lienhard, P. Scholl, D. Barredo, S. Weber, N. Lang, H. P. Büchler, T. Lahaye, and A. Browaeys, “Observation of a symmetry-protected topological phase of interacting bosons with Rydberg atoms,” *Science*, vol. 365, no. 6455, pp. 775–780, 2019.
- [17] D. Genkina, L. M. Ayccock, H.-I. Lu, M. Lu, A. M. Pineiro, and I. Spielman, “Imaging topology of Hofstadter ribbons,” *New Journal of Physics*, vol. 21, no. 5, p. 053021, 2019.
- [18] L. Asteria, D. T. Tran, T. Ozawa, M. Tarnowski, B. S. Rem, N. Fläschner, K. Sengstock, N. Goldman, and C. Weitenberg, “Measuring quantized circular dichroism in ultracold topological matter,” *Nature physics*, vol. 15, no. 5, pp. 449–454, 2019.
- [19] B. S. Rem, N. Käming, M. Tarnowski, L. Asteria, N. Fläschner, C. Becker, K. Sengstock, and C. Weitenberg, “Identifying quantum phase transitions using artificial neural networks on experimental data,” *Nature Physics*, vol. 15, no. 9, pp. 917–920, 2019.
- [20] T. Chalopin, T. Satoor, A. Evrard, V. Makhalov, J. Dalibard, R. Lopes, and S. Nascimbene, “Exploring the topology of a quantum Hall system at the microscopic level,” *arXiv preprint arXiv:2001.01664*, 2020.
- [21] K. Wintersperger, C. Braun, F. N. Ünal, A. Eckardt, M. Di Liberto, N. Goldman, I. Bloch, and M. Aidelsburger, “Realization of anomalous Floquet topological phases with ultracold atoms,” *arXiv preprint arXiv:2002.09840*, 2020.
- [22] N. R. Cooper and J. Dalibard, “Reaching fractional quantum Hall states with optical flux lattices,” *Physical Review Letters*, vol. 110, no. 18, p. 185301, 2013.
- [23] N. Y. Yao, A. V. Gorshkov, C. R. Laumann, A. M. Läuchli, J. Ye, and M. D. Lukin, “Realizing fractional Chern insulators in dipolar spin systems,” *Physical Review Letters*, vol. 110, no. 18, p. 185302, 2013.
- [24] F. Grusdt, F. Letscher, M. Hafezi, and M. Fleischhauer, “Topological growing of Laughlin states in synthetic gauge fields,” *Physical Review Letters*, vol. 113, no. 15, p. 155301, 2014.
- [25] F. Grusdt and M. Hönig, “Realization of fractional Chern insulators in the thin-torus limit with ultracold bosons,” *Physical Review A*, vol. 90, no. 5, p. 053623, 2014.
- [26] Y.-C. He, F. Grusdt, A. Kaufman, M. Greiner, and A. Vishwanath, “Realizing and adiabatically preparing bosonic integer and fractional quantum Hall states in optical lattices,” *Physical Review B*, vol. 96, p. 201103, Nov 2017.
- [27] J. Motruk and F. Pollmann, “Phase transitions and adiabatic preparation of a fractional Chern insulator in a boson cold-atom model,” *Physical Review B*, vol. 96, p. 165107, Oct 2017.
- [28] C. Repellin, T. Yefsah, and A. Sterdyniak, “Creating a bosonic fractional quantum Hall state by pairing fermions,” *Physical Review B*, vol. 96, p. 161111, Oct 2017.
- [29] A. Hudomal, N. Regnault, and I. Vasić, “Bosonic fractional quantum Hall states in driven optical lattices,” *Physical Review A*, vol. 100, no. 5, p. 053624, 2019.
- [30] S. A. Parameswaran, R. Roy, and S. L. Sondhi, “Fractional quantum Hall physics in topological flat bands,” *Comptes Rendus*



- dus Physique*, vol. 14, pp. 816–839, Nov. 2013.
- [31] E. J. Bergholtz and Z. Liu, “Topological flat band models and fractional Chern insulators,” *International Journal of Modern Physics B*, vol. 27, p. 1330017, Sept. 2013.
  - [32] R. Palmer and D. Jaksch, “High-field fractional quantum Hall effect in optical lattices,” *Physical Review Letters*, vol. 96, no. 18, p. 180407, 2006.
  - [33] J. A. Kjäll and J. E. Moore, “Edge excitations of bosonic fractional quantum Hall phases in optical lattices,” *Physical Review B*, vol. 85, no. 23, p. 235137, 2012.
  - [34] W.-W. Luo, W.-C. Chen, Y.-F. Wang, and C.-D. Gong, “Edge excitations in fractional Chern insulators,” *Physical Review B*, vol. 88, no. 16, p. 161109, 2013.
  - [35] F. Grusdt, N. Y. Yao, D. Abanin, M. Fleischhauer, and E. Demler, “Interferometric measurements of many-body topological invariants using mobile impurities,” *Nature Communications*, vol. 7, p. 11994, June 2016.
  - [36] L. Taddia, E. Cornfeld, D. Rossini, L. Mazza, E. Sela, and R. Fazio, “Topological fractional pumping with alkaline-earth-like atoms in synthetic lattices,” *Physical Review Letters*, vol. 118, p. 230402, Jun 2017.
  - [37] X.-Y. Dong, A. G. Grushin, J. Motruk, and F. Pollmann, “Charge excitation dynamics in bosonic fractional Chern insulators,” *Physical Review Letters*, vol. 121, no. 8, p. 086401, 2018.
  - [38] M. Račiūnas, F. N. Ünal, E. Anisimovas, and A. Eckardt, “Creating, probing, and manipulating fractionally charged excitations of fractional Chern insulators in optical lattices,” *Physical Review A*, vol. 98, p. 063621, Dec 2018.
  - [39] R. Umucalılar, E. Macaluso, T. Comparin, and I. Carusotto, “Time-of-flight measurements as a possible method to observe anyonic statistics,” *Physical Review Letters*, vol. 120, no. 23, p. 230403, 2018.
  - [40] C. Repellin and N. Goldman, “Detecting fractional Chern insulators through circular dichroism,” *Physical review letters*, vol. 122, no. 16, p. 166801, 2019.
  - [41] T. Ozawa, H. M. Price, A. Amo, N. Goldman, M. Hafezi, L. Lu, M. C. Rechtsman, D. Schuster, J. Simon, O. Zilberberg, and I. Carusotto, “Topological photonics,” *Reviews of Modern Physics*, vol. 91, no. 1, p. 015006, 2019.
  - [42] P. Knüppel, S. Ravets, M. Kroner, S. Fält, W. Wegscheider, and A. Imamoglu, “Nonlinear optics in the fractional quantum Hall regime,” *Nature*, vol. 572, no. 7767, pp. 91–94, 2019.
  - [43] L. W. Clark, N. Schine, C. Baum, N. Jia, and J. Simon, “Observation of Laughlin states made of light,” *arXiv preprint arXiv:1907.05872*, 2019.
  - [44] S. M. Girvin, “The quantum Hall effect: novel excitations and broken symmetries,” in *Aspects topologiques de la physique en basse dimension. Topological aspects of low dimensional systems*, pp. 53–175, Springer, 1999.
  - [45] J.-y. Choi, S. Kang, S. W. Seo, W. J. Kwon, and Y.-i. Shin, “Observation of a geometric Hall effect in a spinor Bose-Einstein condensate with a skyrmion spin texture,” *Physical Review Letters*, vol. 111, no. 24, p. 245301, 2013.
  - [46] G. Jotzu, M. Messer, R. Desbuquois, M. Lebrat, T. Uehlinger, D. Greif, and T. Esslinger, “Experimental realization of the topological Haldane model with ultracold fermions,” *Nature (London)*, vol. 515, pp. 237–240, Nov. 2014.
  - [47] R. Anderson, F. Wang, P. Xu, V. Venu, S. Trotzky, F. Chevy, and J. H. Thywissen, “Conductivity spectrum of ultracold atoms in an optical lattice,” *Physical Review Letters*, vol. 122, no. 15, p. 153602, 2019.
  - [48] R. J. Fletcher, A. Shaffer, C. C. Wilson, P. B. Patel, Z. Yan, V. Crépel, B. Mukherjee, and M. W. Zwierlein, “Geometric squeezing into the lowest Landau level,” *arXiv preprint arXiv:1911.12347*, 2019.
  - [49] L. J. LeBlanc, K. Jimenez-Garcia, R. A. Williams, M. C. Beeler, A. R. Perry, W. D. Phillips, and I. B. Spielman, “Observation of a superfluid Hall effect,” *Proceedings of the National Academy of Sciences*, vol. 109, no. 27, pp. 10811–10814, 2012.
  - [50] D. R. Hofstadter, “Energy levels and wave functions of Bloch electrons in rational and irrational magnetic fields,” *Physical Review B*, vol. 14, no. 6, p. 2239, 1976.
  - [51] A. S. Sorensen, E. Demler, and M. D. Lukin, “Fractional quantum Hall states of atoms in optical lattices,” *Physical Review Letters*, vol. 94, p. 086803, Mar 2005.
  - [52] A. Dauphin and N. Goldman, “Extracting the Chern number from the dynamics of a fermi gas: Implementing a quantum Hall bar for cold atoms,” *Physical Review Letters*, vol. 111, no. 13, p. 135302, 2013.
  - [53] H. M. Price, O. Zilberberg, T. Ozawa, I. Carusotto, and N. Goldman, “Measurement of Chern numbers through center-of-mass responses,” *Physical Review B*, vol. 93, no. 24, p. 245113, 2016.
  - [54] D. T. Tran, A. Dauphin, A. G. Grushin, P. Zoller, and N. Goldman, “Probing topology by “heating”: Quantized circular dichroism in ultracold atoms,” *Science Advances*, vol. 3, p. e1701207, Aug. 2017.
  - [55] W. Kohn, “Cyclotron resonance and de Haas-van Alphen oscillations of an interacting electron gas,” *Physical Review*, vol. 123, no. 4, p. 1242, 1961.
  - [56] G. Giuliani and G. Vignale, *Quantum theory of the electron liquid*. Cambridge university press, 2005.
  - [57] C. Mudry, *Lecture notes on field theory in condensed matter physics*. World Scientific Publishing Company, 2014.
  - [58] The center-of-mass dynamics of an ensemble of interacting particles in a magnetic field remains classical upon adding a harmonic trap [55, 56].
  - [59] Q. Niu, D. J. Thouless, and Y.-S. Wu, “Quantized Hall conductance as a topological invariant,” *Physical Review B*, vol. 31, pp. 3372–3377, Mar 1985.
  - [60] R. Tao and F. Haldane, “Impurity effect, degeneracy, and topological invariant in the quantum Hall effect,” *Physical Review B*, vol. 33, no. 6, p. 3844, 1986.
  - [61] I. Bloch, J. Dalibard, and W. Zwerger, “Many-body physics with ultracold gases,” *Reviews of Modern Physics*, vol. 80, no. 3, p. 885, 2008.
  - [62] M. E. Tai, A. Lukin, M. Rispoli, R. Schittko, T. Menke, Dan Borgnia, P. M. Preiss, F. Grusdt, A. M. Kaufman, and M. Greiner, “Microscopy of the interacting Harper-Hofstadter model in the two-body limit,” *Nature (London)*, vol. 546, pp. 519–523, June 2017.
  - [63] M. Hafezi, A. S. Sørensen, E. Demler, and M. D. Lukin, “Fractional quantum Hall effect in optical lattices,” *Physical Review A*, vol. 76, p. 023613, Aug 2007.
  - [64] Due to the gapless nature of the edge states,  $N_0(\alpha)$  is only defined approximately;  $N_0(\alpha)$  may be more formally defined by considering the states with an energy no larger than  $E_{\min}(\alpha) + w(\alpha)$  where  $E_{\min}(\alpha)$  is the lowest single-particle energy and  $w(\alpha)$  is the bandwidth of the lowest band in the case of periodic boundary conditions.
  - [65] We refer here to the infinite plane geometry, where the FQH droplet is confined through total angular momentum conservation, not by the addition of a confinement potential.
  - [66] see *Supplementary Material*.
  - [67] The  $\nu = 2/3$  Jain fraction is a possible candidate among these phases [33, 77], but we did not identify any clear topological signature of this phase in our setting.

- [68] In the continuum, a hard confinement was shown to have a drastic influence on the energy of edge modes [78, 79].
- [69] A. Sterdyniak, N. Regnault, and B. A. Bernevig, “Extracting excitations from model state entanglement,” *Physical Review Letters*, vol. 106, p. 100405, Mar 2011.
- [70] F. D. M. Haldane, ““Fractional statistics” in arbitrary dimensions: A generalization of the Pauli principle,” *Physical Review Letters*, vol. 67, pp. 937–940, Aug 1991.
- [71] D. J. Thouless, M. Kohmoto, M. P. Nightingale, and M. den Nijs, “Quantized Hall conductance in a two-dimensional periodic potential,” *Physical Review Letters*, vol. 49, no. 6, p. 405, 1982.
- [72] M. Kohmoto, “Zero modes and the quantized Hall conductance of the two-dimensional lattice in a magnetic field,” *Physical Review B*, vol. 39, no. 16, p. 11943, 1989.
- [73] R. Bianco and R. Resta, “Mapping topological order in coordinate space,” *Physical Review B*, vol. 84, no. 24, p. 241106, 2011.
- [74] D.-T. Tran, A. Dauphin, N. Goldman, and P. Gaspard, “Topological Hofstadter insulators in a two-dimensional quasicrystal,” *Physical Review B*, vol. 91, no. 8, p. 085125, 2015.
- [75] N. H. Lindner, A. Auerbach, and D. P. Arovas, “Vortex quantum dynamics of two dimensional lattice bosons,” *Physical Review Letters*, vol. 102, no. 7, p. 070403, 2009.
- [76] J. Motruk and I. Na, “Detecting fractional Chern insulators in optical lattices through quantized displacement,” *arXiv:2005.XXXXX*, 2020.
- [77] G. Möller and N. R. Cooper, “Composite fermion theory for bosonic quantum Hall states on lattices,” *Physical Review Letters*, vol. 103, p. 105303, Sep 2009.
- [78] R. Fern and S. H. Simon, “Quantum Hall edges with hard confinement: Exact solution beyond Luttinger liquid,” *Physical Review B*, vol. 95, p. 201108, May 2017.
- [79] E. Macaluso and I. Carusotto, “Hard-wall confinement of a fractional quantum Hall liquid,” *Physical Review A*, vol. 96, p. 043607, Oct 2017.
- [80] S. Powell, R. Barnett, R. Sensarma, and S. D. Sarma, “Bogoliubov theory of interacting bosons on a lattice in a synthetic magnetic field,” *Physical Review A*, vol. 83, no. 1, p. 013612, 2011.
- [81] T. Ozawa, H. M. Price, and I. Carusotto, “Momentum-space Harper-Hofstadter model,” *Physical Review A*, vol. 92, no. 2, p. 023609, 2015.

## Supplementary material

### Ramps used in our calculations

In the Hall-drift protocol described in the main text, the force  $F(t)$  and the tunneling terms  $J(r, t)$  are slowly ramped up until reaching a stationary regime at  $t = \tau_{\text{ramp}}$ ; here  $r$  denotes the radial coordinate on the 2D plane. In our numerical calculations, the force is ramped up according to the first-order smoothstep function

$$F(t) = F \left( 3 \left( \frac{t}{\tau_{\text{ramp}}} \right)^2 - 2 \left( \frac{t}{\tau_{\text{ramp}}} \right)^3 \right), \quad (2)$$

while we have used an exponential ramp for the tunneling terms,

$$J(r, t) = J \exp \left( -\frac{r - R_0}{R_1} \left( \frac{\tau_{\text{ramp}}}{t} - 1 \right) \right), \quad (3)$$

where  $R_0$  is the radius of the small circular box where the initial state is prepared, and  $R_1$  is the radius of the larger circular box (i.e. the simulation box) into which it is released. These ramps were used both for the hardcore-boson and non-interacting-fermion cases (main text). We expect that the exact form of the ramps should not be crucial in view of reaching a stationary regime, as long as they are smooth enough.

### Single-particle Hofstadter spectrum in a small circular box

We show the single-particle Hofstadter spectrum for a lattice of  $N_s = 60$  sites in Fig. 5, for three representative values of the flux  $\alpha$ . To label the eigenstates, we use the eigenvalues of the  $C_4$ -rotation operator; in this system with discrete rotational symmetry [80, 81], they are equivalent to the angular momentum modulo 4.

Considering this lattice of  $N_s = 60$  sites and a flux  $\alpha \approx 0.2$ , we have shown that the ground state of  $N = 4$  hardcore bosons can be identified as a  $\nu = 1/2$  FCI ground state (see main text). In this setting, only the 7 lowest-energy orbitals have a substantial occupation in this ground state [see Fig. 2(c) of the main text]. In Fig. 5, we show that these 7 orbitals form the nearly-flat lowest band of the single-particle spectrum at  $\alpha = 0.2$ .

### Ground state properties and Hall drifts for additional system sizes

In the main text, we have shown numerical data for  $N = 4$  hardcore bosons prepared in a circular box of  $N_s = 60$  sites. We have obtained consistent results for other particle numbers  $N$  and lattice sizes  $N_s$ , (corresponding to other densities  $\rho$ ), which we present in this Appendix. For each number of

particles ( $N = 3, 4$ ), we show the results for the smallest system where Hall-drift signatures of a  $\nu = 1/2$  FCI state were found:  $N_s = 40$  for  $N = 3$  and  $N_s = 49$  for  $N = 4$ . Besides, we have verified that the linear-response regime is reached when using a weak force  $F \lesssim 0.01J/d$ . The results presented in this Appendix correspond to setting  $F = 0.0001J/d$ .

Figure 6 shows the ground-state properties and the center-of-mass Hall drift for  $N = 4$  bosons and  $N_s = 49$  sites. Based on the low-energy spectra and entanglement spectroscopy, we find clear signatures of the  $\nu = 1/2$  FCI state for  $0.18 \leq \alpha \leq 0.29$ . We point out that this shift of the FCI phase towards larger values of  $\alpha$  compared to the case presented in the main text ( $N = 4$ ,  $N_s = 60$ , where the FCI regime corresponds to  $0.15 \leq \alpha \leq 0.25$ ; see Fig. 2 in the main text) is consistent with a larger particle density  $\rho = N/N_s$ . We observe a decreased sensitivity of the Hall conductivity in a large flux window, which is included in the FCI regime. We note that the width of this emergent “plateau”, as defined by the two inflection points located at the boundaries of this window, is slightly smaller than the FCI region; as shown in the main text (using  $N_s = 60$  sites for  $N = 4$  bosons), this discrepancy is reduced by increasing the system size, which suggests that it is due to the smallness of this minimal setting ( $N_s = 49$  sites for  $N = 4$  bosons).

For  $N = 3$  bosons, the particle entanglement spectrum (PES) cannot provide a topological signature of the FCI. Indeed the PES that results from the only available particle bipartition ( $2 + 1$ ) corresponds to the spectrum of the single-particle density matrix (which cannot probe topological order). Nevertheless, for  $N = 3$  bosons and  $N_s = 40$  sites, the low-energy many-body spectrum and the orbital occupation are compatible with a FCI state in the flux window  $0.16 \leq \alpha \leq 0.28$ , where the Hall drift simulation reveals an emergent Hall plateau; see Fig. 7.

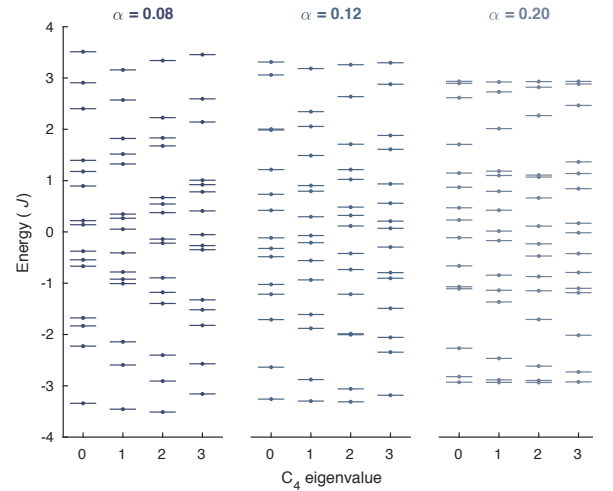


Figure 5. Single-particle spectrum for  $N_s = 60$  sites and flux density  $\alpha = 0.08, 0.12$  and  $0.2$ , labeled according to the eigenvalues of the  $C_4$ -rotation operator. The occupation of each of these orbitals in the  $N = 4$  hardcore-boson configuration is given in Fig. 2(c) of the main text.



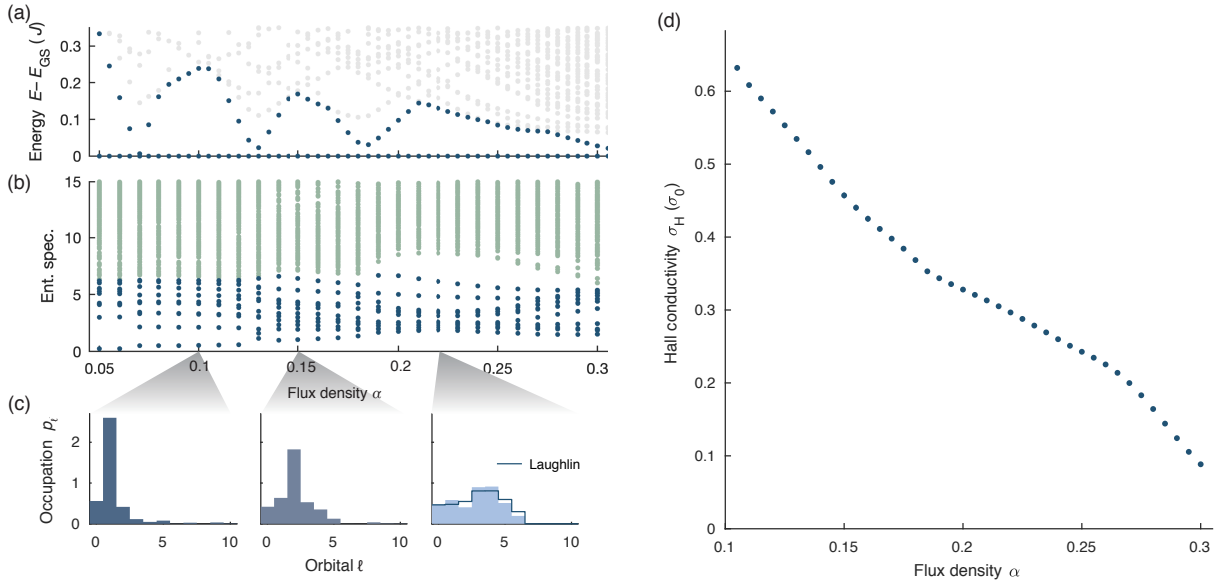


Figure 6. Properties of a system of  $N = 4$  hardcore bosons in a circular box of  $N_s = 49$  sites in the Harper-Hofstadter-Hubbard model. The left column shows the characterization of the ground state through static signatures (following Fig. 2 of the main text): (a) Energy spectrum; (b) Particle Entanglement Spectrum; (c) Occupation of the single-particle orbitals in the ground state, in increasing energy order (the line shows the orbital occupation for the  $N = 4$  Laughlin state on the disk, where the orbitals are sorted in increasing angular momentum); (d) Hall conductivity as extracted from the COM Hall drift upon releasing the ground state into a circle with 113 sites and applying a force  $F = 0.0001J/d$ .

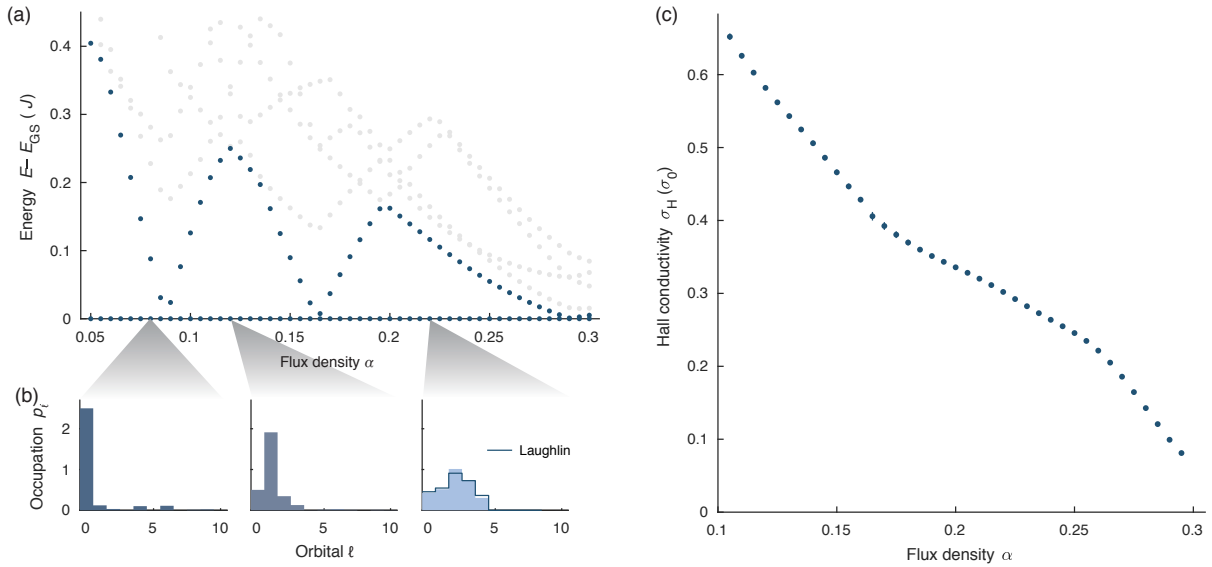


Figure 7. Properties of a system of  $N = 3$  hardcore bosons in an elliptic box of  $N_s = 40$  sites in the Harper-Hofstadter-Hubbard model. The left column shows the characterization of the ground state through static signatures: (a) Energy spectrum; (b) Occupation of the single-particle orbitals in the ground state, in increasing energy order (the line shows the orbital occupation for the  $N = 3$  Laughlin state on the disk, where the orbitals are sorted in increasing angular momentum); (c) Hall conductivity as extracted from the COM Hall drift upon releasing the ground state into an ellipse with 100 sites and applying a force  $F = 0.0001J/d$ .